Effects of land-use patterns at different scales on water quality in the Huaihe River Basin in China

Lin Wu[1], Xiaolong Li[1*], Liangmin Gao[1,3], Kai Zhang[1], Zhendong Pang[2]

[1]School of Earth and Environment, Anhui University of Science & Technology, Huainan 232001, China

[2]Huainan Ecological and Environmental Monitoring Center of Anhui Province ,Huainan 232001, China

[3]Anhui Lida Earth and Environment Technology Co, Ltd，Huainan 232001, China

*to whom all correspondence should be addressed : e-mail : lxl0994@163.com; Contact number: 0554-6668430

Graphical abstract

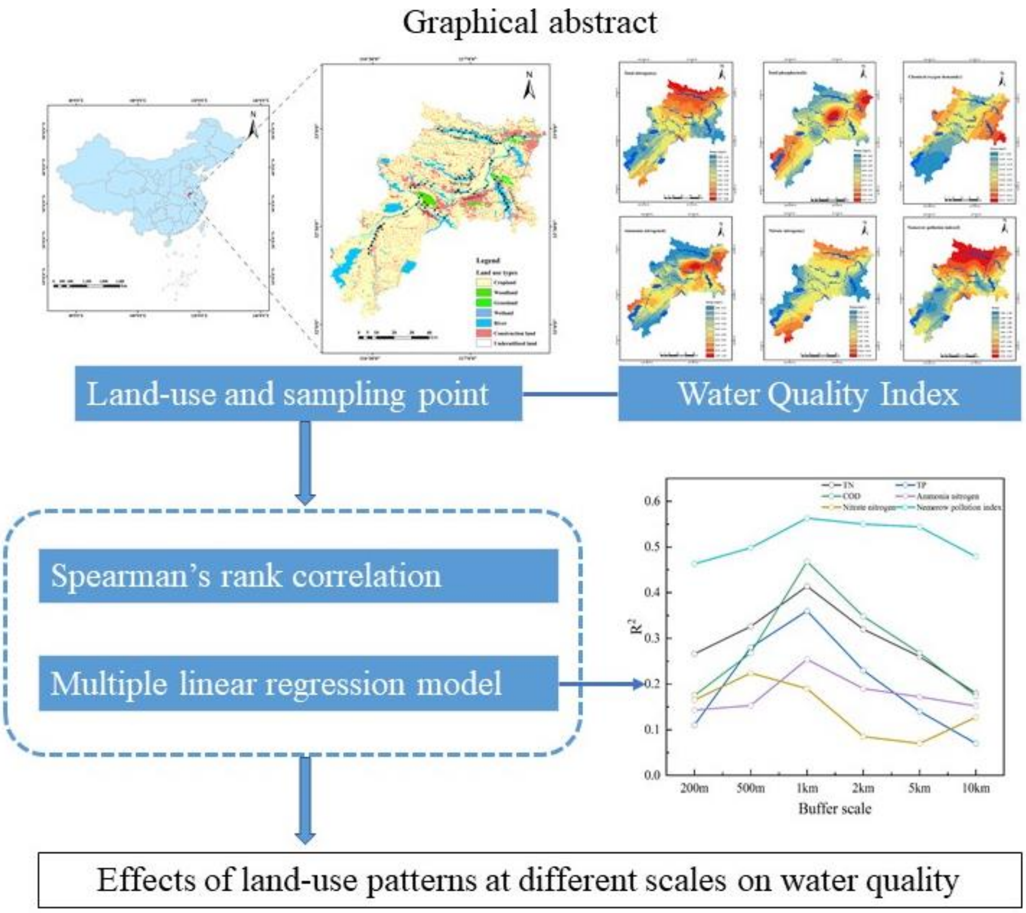

ABSTRACT

The influence of land-use patterns on water quality in the Huaihe River Basin was analyzed using the Nemerow index, correlation and multiple linear regression analysis based on the measured data from 62 sampling sites in the Huaihe River Basin (China). In the point buffer zone, a significant correlation was observed between land-use patterns at different buffer zone scales and water quality parameters. Cultivated land and construction land are significantly positively correlated with all water quality parameters, while forest land and grassland were negatively correlated with all water quality parameters. The 1km buffer zone exhibited the greatest interpretation of TN, TP, COD, NH_4^+-N and the Nemerow index, while the 500m buffer zone exhibited the greatest interpretation of NO_3^--N. These findings indicate that forest land and grassland were the main land-use types for the interception and consumption of pollutants. While cultivated land and construction land served as ' source of TN, TP, COD, NH_4^+-N and NO_3^--N. These findings show that controlling land-use patterns on a small-scale (≤ 1 km) land-use pattern, especially the proportion of cultivated land and construction land, can be an effective tool for the protection of water quality basin areas.

Keywords : land-use ; spatial scale ; Nemerow index ; correlation ; Huaihe River Basin ;

1. Introduction

Water is a fundamental resource required for the survival and development of all biological organisms, including humans(Prasad et al., 2024; Venkatraman et al., 2025), In light of the escalating water resource scarcity in the 21st century, it is imperative to take immediate action to safeguard the existing water resources(Maruthai et al., 2025; Selvanarayanan et al., 2024). Rivers are the most directly available freshwater resource on Earth, and river water quality is an important indicator of watershed ecosystem health. River water quality can be affected by various natural and anthropogenic factors. including rainfall, geology, topography, soil type, climate conditions, vegetation, urbanization, and industrial or agricultural activities, particularly within basin areas(Bouchareb et al., 2024; Kamaruddin et al., 2015; Mahdiani et al., 2016). Various studies have shown that changes in land-use type and structure can provide an intuitive reflection of the impact of human activities on the ecological environment, with the corresponding impact on non-point source pollution within basin areas, being a main factor contributing to changes in river water quality(Goodarzi et al., 2023; Hong et al., 2016; Wang et al., 2023a; Zhang et al., 2021). Therefore, it is essential that the relationship between land-use patterns and watershed water quality is examined for effective land-use management planning and the protection of aquatic ecological environments and resources.

In recent years, the rapid development of geographic information system (GIS) and remote sensing (RS) technologies, have resulted in an abundance of watershed studies showing correlations between land-use patterns and river water quality. Various studies have shown that significant correlations exist between land-use patterns and the regional water environment. In terms of research scope, previous studies have mainly covered several zone types, such as the watershed, sub-watershed, river buffer zone and point buffer zone areas. For example, Wang et al(Wang et al., 2024). used redundancy analysis to analyze the relationship between land-use models and river water quality parameters at the river section scale and seasonal scale. Chen et al(Chen et al., 2020). used GIS and regression analysis to explore the relationship between land-use changes and surface water quality indices in the Mitiga Basin. Mei et al(Xiao-Mei et al., 2023). used the investment model to calculate the impact of land-use transformation on water quality in the Ciyao River Basin. Mu et al(Mu et al., 2023). used redundancy, multiple linear regression and Spearman’s correlation analysis to study the impact of land-use types at different buffer scales, on water quality in the middle section of the Huaihe River Basin. Tan et al(Tan et al., 2024). used correlation and redundancy analysis to explore the impact of land-use composition on water quality at different spatial and temporal scales.

The Huaihe River Basin is located in Eastern China, with the main land-use types being typical agricultural production and industrial development, showing that with the rapid development of a regional social economy, land-use types along the Huaihe River are gradually changing, and the scale effect of land use types on the surface water environment is a critical area of concern for ecological environmental protection.(He et al., 2023; Liang et al., 2021; Wang et al., 2018), which is a critical area of concern in ecological and environmental protection. To ensure the safety of the water environment in the Huaihe River Basin, this study selects the Huaihe River Basin as the research subject. Based on remote sensing imagery, land use types are extracted, and combined with surface water quality monitoring results, the relationship between land use types and the water environment in the Huaihe River Basin is analyzed. The study explores the impact mechanisms of different land use types on the water environment in the Huaihe River Basin, aiming to provide a scientific basis for sustainable watershed management and the construction of an ecological security barrier in the Huaihe River Basin, or similar environments worldwide.2 Materials and methods

2.1 Overview of the study area

The study area was located in the middle section of Huaihe River Basin (Anhui area), which was located between 111° 55 ' -121° 20 ' E and 30° 55 ' -36° 20 ' N, as shown in Figure. 1. This region has an average annual precipitation of 913.6 mm, with rainfall distributed more in the south than in the north, with an uneven spatial and temporal distribution(Xu et al., 2023; Xu et al., 2019b). Within the study area, the north bank of the Huaihe River has a flat region of the Huaibei Plain, while south of the Huaihe River has a hilly terrain. The main land-use type was cultivated land, accounting for 70.84% of the total area of the study area, while forest land, grassland, construction land and water bodies accounted for 0.93 %, 1.14 %, 15.70 % and 9.85 % of the total study area, respectively.

2.2 Collection and processing of water quality data

In this study, two field surveys were conducted along the main stream and main tributaries of the Huaihe River during the dry season (January 2021), with the distribution of the 62 sampling points shown in Figure. 1. Samples were stored in a high-density polyethylene container and were stored at 4 °C. Water quality parameters were measured, such as total nitrogen (TN), total phosphorus (TP), ammonium nitrogen (NH_4^+-N), nitrate nitrogen (NO_3^--N) and COD, with the specific determination methods used shown in Table 1. The equipment required for the experiment is listed in Table 2.

Table 1 Determination method used for each water quality index parameter

Index	Assay method
TN	Alkaline potassium persulfate digestion UV spectrophotometry (HJ 636-2012)
TP	Ammonium molybdate spectrophotometric method (GB 11893-89)
COD	Potassium dichromate rapid digestion-photometry (HJ 924-2017)
NO_3^--N	Ultraviolet spectrophotometry (HJ/T346-2007)
NH_4^+-N	Nessler's reagent spectrophotometry (HJ 535-2009)

Table 2 Laboratory Instruments

Serial Number	Instrument	Model	Manufacturer
1	Ultraviolet Spectrophotometer	N5000PLUS	Shanghai Youke Instrument and Meter Co., Ltd.
2	High-pressure Steam Sterilizer	DGL-50B	Jiangsu Dengguan Medical Equipment Co., Ltd.
3	8-Well Microcrystalline COD Digester	SH-108	Jiangsu Haihuan Instrument Equipment Co., Ltd.
4	UPR Ultra Pure Water System	UPI-I-5T	Chengdu Tangning Kangning Technology Development Co., Ltd.

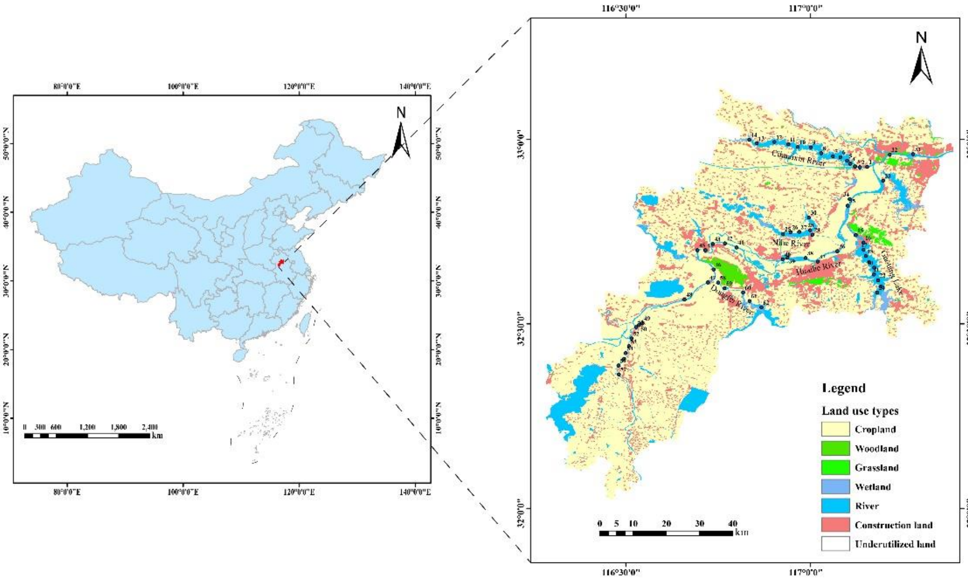

Figure 1 Map of the study area, showing the land-use map and sampling point distribution

Previous studies have shown that land-use patterns within the 200 m～ 10 km buffer zone have a significant impact on river water quality(Dai et al., 2024; Xu et al., 2019a; Xu et al., 2021). In order to study the influence of land-use patterns at different buffer zone scales on water quality in the Huaihe River Basin, buffer zones with radii of 200 m, 500 m, 1 km, 2 km, 5 km and 10 km were compared, with each sampling point as the center. The land-use types were divided into six categories, including cultivated land, water area, construction land, wetlands, forest land and grassland. The area of each land-use type within the buffer zone was determined and the relative proportion that each land-use type accounted for was calculated.

2.3 Analysis methods

Firstly, the Kriging interpolation was used to construct the spatial distribution map of surface water pollutant concentrations and establish the Nemerow index value for the area. The Nemerow pollution index was used to analyze regional changes in water quality throughout the Huaihe River Basin area. Secondly, Spearman's rank correlation coefficients were determined between the relative proportion of each land-use type area and different water quality parameters at various buffer zone scales. The proportion of land-use type area at different buffer zone scales was used as an explanatory variable and each water quality parameter was used as a response variable for the construction of a multiple linear regression model, the adjusted R^2 value of the model represents the degree to which land use patterns explain the water quality parameters.Using this method, the effects of land-use structure on the water quality of the main stream and main tributaries of the Huaihe River were calculated at different buffer zone scales. Microsoft Excel 2019 and SPSS Statistics 27 were employed for data analysis and processing. Statistical graphics were generated using Origin 2021, ArcMap 10.8, and Adobe Illustrator 2023. Specifically, ArcMap 10.8 was utilized to extract the areas of land use types within different buffer zones and to simultaneously create land use maps and Kriging interpolation maps. Additionally, SPSS Statistics 27 was applied to calculate the Spearman correlation coefficients between each water quality parameter and the proportions of land use types, as well as to construct a multiple linear regression model. The land-use map used in these studies originated from the Resource and Environmental Science Data Center of the Chinese Academy of Sciences (http://www.resdc.cn).

Constructing a multiple linear regression model of water quality and land use types can help us understand the impact of different land use types on water quality. The model formula is shown in Equations (1):

$$\boldsymbol{Y} = \boldsymbol{\alpha} \cdot (\boldsymbol{\beta_1 X_1} + \boldsymbol{\beta_2 X_2} + \boldsymbol{\beta_3 X_3} + \boldsymbol{\beta_4 X_4} + \boldsymbol{\beta_5 X_5} + \boldsymbol{\beta_6 X_6}) \qquad (1)$$

Where, Y represents the measured water quality index in the watershed; α is a constant; $\boldsymbol{\beta_1 \sim \beta_6}$ are the correlation coefficients between the area proportions of the five land use types (crop land, woodland, grassland, wetland, river, and construction land) and the water quality index, respectively;

$\boldsymbol{X_1 \sim X_6}$ represent the six land use types (crop land, woodland, grassland, wetland, river, and construction land).

The Nemerow index method can not only highlight the most serious pollution factors, but also takes into account other evaluation factors that may be more suitable, to a certain extent. In addition, the Nemerow index method can avoid the subjective influence of artificially assigning a weight to each factor during the calculation process(Su et al., 2022a; Su et al., 2022b). In the present study, TN, TP and COD were used to calculate the Nemerow index, according to Equations (2)-(4), as follows:

$$I_i = \frac{C_i}{C_{oi}} \tag{2}$$

$$\bar{I} = \frac{1}{n}\sum_{i=1}^{n} I_i \tag{3}$$

$$I_p = \sqrt{\frac{I_{i,max}^2 + \bar{I}^2}{2}} \tag{4}$$

Where, I_i represents the pollution index of the first evaluation factor; $\bar{I}$ represents the average value of the pollution index of n evaluation factors; I_p represents the Nemerow pollution index value; $I_{i,max}$ is the maximum pollution index value in all pollution evaluation factors; C_i is the measured value of the first evaluation factor; C_{oi} is the water quality standard value for the evaluation factor i (specific grading degrees shown in Table 3) (Wang et al., 2022). This study did not consider the functional classification of surface water quality categories and C_{oi} adopted the 'Surface Water Environmental Quality Standard' (GB 3838-2002) III standard.

Table 3 Water quality level based on Nemerow pollution index method

Class of pollution	Nemerow index	Pollution level
1	$I_p \leq 1$	Cleaning
2	$1 < I_p \leq 2$	Light pollution
3	$2 < I_p \leq 3$	Moderate pollution
4	$3 < I_p \leq 4$	Heavy pollution
5	$4 < I_p \leq 5$	Serious pollution

3 Results analysis and discussion

3.1 Land-use structure at different buffer zone scales

For each sampling point, the relative proportion of each land-use type within buffer zone areas of 200 m, 500 m, 1 km, 2 km, 5 km and 10 km is shown in Figure 2. The area consisting of river, cultivated land and construction land was relatively large, while the area consisting of other land-use types was relatively small. The sampling points were mainly surrounded by rivers, cultivated land and construction land. The proportion of cultivated land and construction land increased at larger spatial scales, while the proportion consisting of rivers decreased at larger spatial scales.

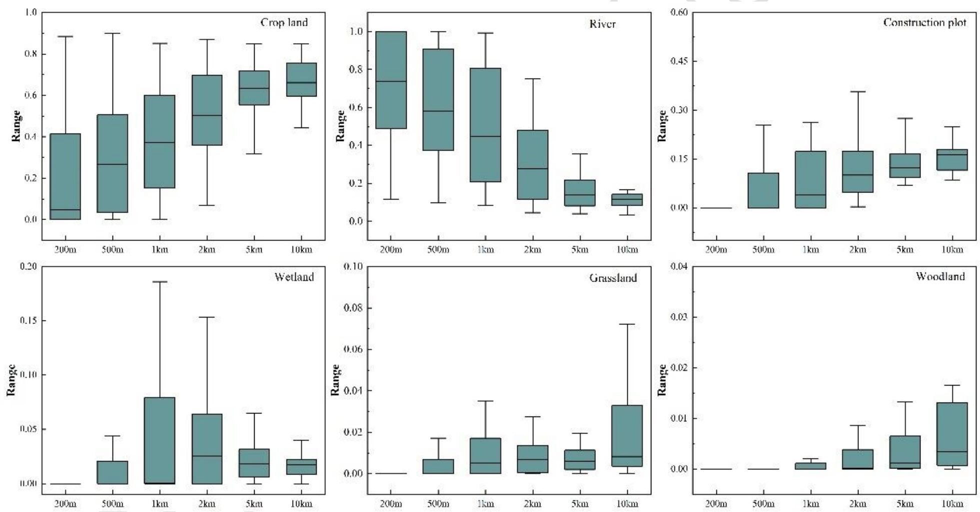

Figure 2 The relative proportion of land-use types within the study area at different buffer zone scales

3.2 Spatial variation in water quality index values

The descriptive statistics of water quality indicators for the Huai River Basin are presented in Table 4. The spatial distribution of TN concentrations across the Huaihe River Basin varied significantly. TN concentrations across the study area mainly exhibited a trend of higher concentrations in the north of the study area and lower concentrations in the south, while in the central area along the Huaihe River TN concentrations were in the mid-level (Figure. 3a). As shown in Figure.

3b, the TP concentrations within the study area mainly exhibited a trend of higher TP concentrations in the upper and lower reaches of the study area and lower concentrations in the central region. Similarly, COD concentrations exhibited an overall trend of higher concentrations in the north of the study area and lower concentrations in the south (Figure. 3c), while the mass concentration of NH_4^+-N mainly exhibited a trend of higher concentrations in the upper and lower reaches of the study area and lower concentrations in the central region (Figure. 3d). Finally, it can be seen from Figure. 3e, that the concentration of NO_3^--N mainly exhibited a trend of higher concentrations in the north and lower concentrations in the south, with concentrations in the main stream of the central Huaihe River remaining at a mid-level. Finally, as can be seen from Figure 3f, Nemerow pollution index concentration also predominantly displays a trend of being higher in the north and lower in the south, with the central section of the main stem of the Huai River at a moderate level. A comparison of Figure. 3a and Figure. 3f showed that the Nemerow pollution index distribution was similar to that of TN, which indicates that TN is an important factor affecting water quality in Huaihe River Basin.

Table 4 Descriptive statistics for water quality indicators in the ($mg \cdot L^{-1}$)

Parameter	Maximum value	Minimum value	Mean value	Standard deviation
TN ($mg \cdot L^{-1}$)	5.46	0.61	2.78	1.52
TP($mg \cdot L^{-1}$)	0.72	0.03	0.14	0.12
NO_3^--N($mg \cdot L^{-1}$)	4.72	0.12	1.78	1.54
NH_4^+-N($mg \cdot L^{-1}$)	1.56	0.05	0.33	0.27
COD($mg \cdot L^{-1}$)	47	7	19	10

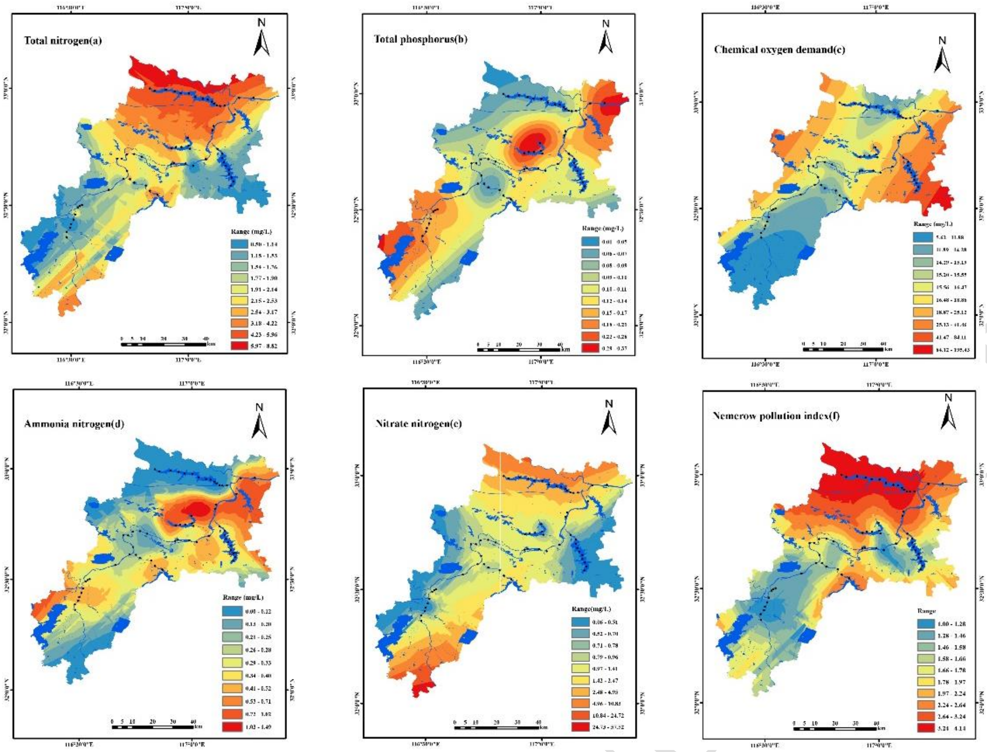

Figure 3 Distribution of pollutant concentrations and water quality index parameters at sampling points across the Huaihe River Basin study area

3.3 Watershed pollution index characteristics

The distribution of the Nemerow index in the Huaihe River Basin is shown in Figure. 4(The calculation method is shown in Equations (2)-(4)). The mean Nemerow index value across the basin area was 2.3, with a variation range of 0.7～4.2. The Nemerow index values in the Cihuaixin River (the first tributary of the Huaihe River) ranged from 3～4, while in the lower reaches of Huaihe River in the study area ranged from 2～3, the Nemerow index of the upper reaches of Huaihe River in the study area ranged from 1～2 and the Nemerow index of Gaotang Lake and the Nihe River ranged from 1～2. Among these, the Nemerow pollution index values in the lower reaches of the main stream of the Huaihe River fluctuated greatly, while the degree of fluctuation in the upper reaches and tributaries were relatively small.

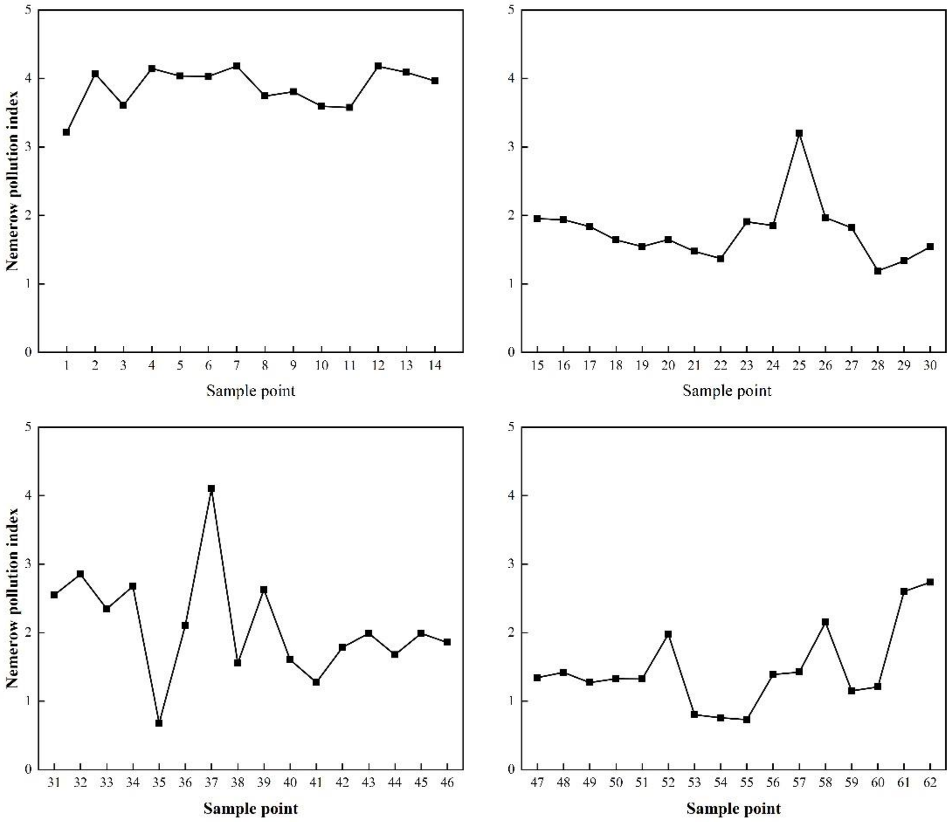

Figure 4 Nemerow pollution index value distribution throughout the Huaihe River Basin

3.4 The correlation between land-use types and water quality in the basin

At different buffer-zone scales, TN was significantly negatively correlated with cultivated land, while being significantly positively correlated with grassland, wetlands, rivers and construction land (Table 5). Among these, the correlation with grassland within a 1 km buffer zone was the highest ($r = 0.547$, $P < 0.01$). TP was significantly negatively correlated with forest land, wetlands and river, while being significantly positively correlated with cultivated land and construction land, among which the highest correlation was with rivers within a 200 m buffer zone ($r = -0.419$, $P < 0.01$). A significant negative correlation existed between COD and both cultivated land (200 m～1 km) and construction land (2 km～5 km), while significant positive correlations existed between COD and forest land (10 km), wetlands (200 m～500 m) and rivers (200 m～10 km). Among these, the correlation was highest between COD and rivers within the 5 km buffer zone area ($r = -0.416$, $P < 0.01$). NH_4^+-N was significantly negatively correlated with rivers (200 m～ 2 km) and forest land (5 km), while being significantly positively correlated with cultivated land and construction land. Among these, the correlation between NH_4^+-N and rivers was highest within the 200 m buffer zone area ($r = -0.422$, $P < 0.01$). A significant positive correlation existed between NO_3^--N and both grassland (500 m～5 km) and construction land (500 m～ 2 km), with the highest correlation observed with grassland within the 1 km buffer zone ($r = 0.539$, $P < 0.01$). The Nemerow pollution index was significantly negatively correlated with cultivated land and exhibited a high correlation with cultivated land (200 m～500 m) ($r < -0.6$, $p < 0.01$), while being significantly positively correlated with grassland, wetlands, rivers and construction land, with the highest correlation observed with river areas (500 m ～5 km) ($r > 0.6$, $p < 0.01$).

Table 5 Relationships between water quality parameters and land-use types at various buffer zone scales, based on Spearman's rank correlation coefficient data

Water quality parameter	Buffer zone scale	Land-use type					
		Cropland	Woodland	Grassland	Wetlands	River	Construction land
TN	200m	0.278*			0.263**	0.266*	
	500m	0.209*		-0.307*	0.270*	0.274*	0.253*
	1km	0.216*		-0.547**		0.277*	0.283*
	2km			-0.510**			0.227*
	5km		-0.269*	-0.539**			
	10km			-0.255*			
TP	200m	0.290*			0.278*	0.419**	0.275*
	500m	0.225*			0.238*	-0.285*	0.266*
	1km	0.203*				-0.220*	
	2km						
	5km		-0.339*				
	10km		-0.301*				
COD	200m	-0.355**			0.362**	0.335*	
	500m	-0.287*			0.302*	0.317*	
	1km	-0.296*				0.355**	
	2km					0.297*	0.297*
	5km					0.331**	0.416**
	10km		-0.317*			0.271*	
NH_4^+-N	200m	0.254*				-0.422*	0.314*
	500m	0.240*				-0.316*	0.209*
	1km					-0.208*	
	2km					-0.253*	
	5km		-0.281*			-0.256*	
	10km						
NO_3^--N	200m						
	500m			-0.337**			0.420**
	1km			-0.539**			0.324*
	2km			-0.500**			0.249*
	5km			-0.475**			
	10km						
Nemerow pollution index	200m	0.635**			0.366**	0.528**	
	500m	0.612**			0.544**	0.639**	0.481*
	1km	0.583**			0.542**	0.675**	0.463*
	2km	0.439**		-0.298*		0.617**	0.431**
	5km	0.331*		-0.446**		0.617**	0.284*
	10km			-0.530**		0.461**	

Note: Only explanatory variables with significant correlations were listed. * indicates P < 0.05; ** indicates P < 0.01.

Multivariate linear regression analysis showed that the influence of land-use patterns on water quality parameters increased initially and then decreased with increasing buffer zone scale (Figure 5). The R^2 values generated from the multiple regression model of TN, TP, COD, NH_4^+-N and the Nemerow pollution index reached a maximum level within the 1 km buffer zone, reaching 0.414, 0.36, 0.468, 0.254 and 0.563, respectively ($P < 0.01$). The R^2 value of the NO_3^-N multiple linear regression model reached a maximum level within the 500 m buffer zone of 0.224 ($P < 0.01$). The land-use patterns within the large-scale buffer zone area (5 km ～ 10 km) provided a relatively weak explanation for the spatial distribution of water quality parameters. In general, land-use types explained the spatial differentiation of the Nemerow pollution index more than other parameter, while the association between land-use types and NO_3^--N concentrations was the lowest.

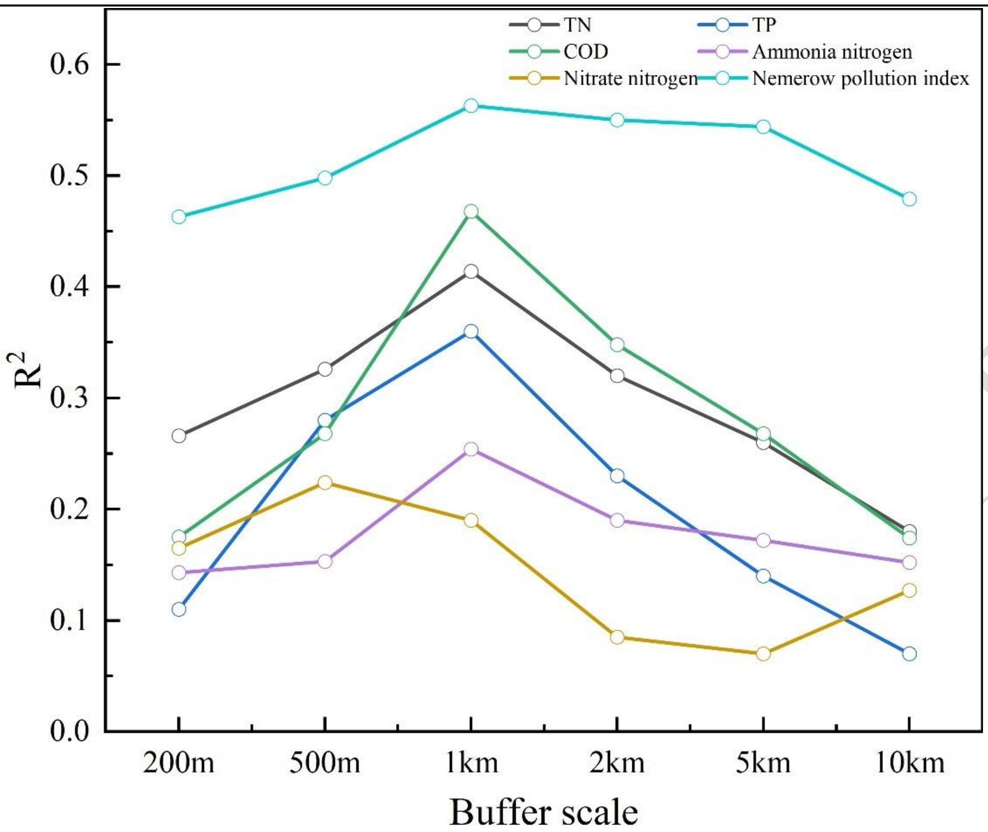

Figure 5 The explanatory power of different water quality parameters based on the multiple linear regression model (R^2 value) data for land-use patterns at different buffer zone scales.

3.5 Discussion

Based on the combined analysis of land-use and pollutant distribution maps (Figure. 1 and Figure. 3), the northern part of the study area (mostly cultivated land and construction land) was shown to be highly affected by frequent anthropogenic activities, with regional rivers greatly disturbed(Wang et al., 2023b; Yang et al., 2023). The TN, NO_3^--N and Nemerow index values were relatively high. Furthermore, in the dry season, the amount of rainwater replenishment was small in the north of the study area and the self-purification capacity of water bodies was poor. In contrast, the concentration of pollutants in forest and grassland areas in the central and southern regions of the study area was relatively low and the vegetation coverage of forest and grassland areas was higher than other land-use types. In the dry season, abundant plant root growth reduced pollutant migration through surface runoff due to factors such as plant root absorption and soil retention, effectively intercepting pollutants and reducing their transfer to rivers, reducing the scale of disturbance to the river water body(Wu et al., 2021; Zhang et al., 2023).

TN, TP and NH_4^+-N concentrations were significantly positively correlated with cultivated land within a 1 km buffer zone (Table 5), which was attributed to agricultural activities and the excessive use of pesticides and fertilizers, with the unabsorbed fractions of pollutants flowing into the water body with the slope water, causing a reduction in water quality(Zhang et al., 2022). However, a poor correlation was observed with cultivated land within a larger buffer zone(2km～10km), which may be due to cultivated land accounting for a small proportion of the large-scale buffer zone, while pollutant may also be adsorbed and deposited during transport over a larger scale. COD exhibited a significant negative correlation with cultivated land within a 1 km buffer zone, showing that cultivated land played a role as a COD sink. A significant negative correlation existed between TN, TP, COD, NH_4^+-N and woodlands within the large-scale buffer zone(5km～10km). There was a significant negative correlation observed between TN, NO_3^--N and grasslands within a 5 km buffer zone, due to forest land and grasslands being rich in vegetation, reducing pollutant migration through surface runoff and mitigating water pollution through biochemical effects such as vegetation root absorption and soil retention(Li et al., 2019). TN, TP and COD were positively correlated with wetlands in small-scale buffer zones(200m,500m), which may be due to the decomposition of aquatic plants in wetlands during winter, resulting in an increase in pollutant concentrations within the basin area. There was a significant positive correlation between TN, COD and rivers within a 1km buffer zone, which may be due to cultivated land and construction land and other exogenous inputs. TP and NH_4^+-N were significantly negatively correlated with rivers in small-scale buffer zones(200m～1km), which may be due to the self-purification function of the river itself. TN, TP, COD, NH_4^+-N and NO_3^--N were significantly positively correlated with construction land, due to the high-intensity of anthropogenic activities in construction areas, producing domestic sewage and industrial wastewater, thereby affecting water quality(Yao et al., 2023).

The Nemerow index was significantly positively correlated with cultivated land within a 500m～5km buffer zone, wetlands, water bodies and construction land, indicating that agricultural source pollution, residential sewage discharge, wetland litter degradation and river exogenous pollutant invasion were the main causes of watershed pollution within the study area. There was a significant negative correlation observed with grassland within a 2km～10km buffer zone, indicating that grassland can effectively intercept and absorb pollutants.

Multivariate linear regression analysis showed that land-use types had the highest explanatory power for the Nemerow pollution index and the lowest explanatory power for NO_3^- N pollution. Multivariate linear regression was performed to interpret the effects of land-use patterns on water quality parameters, exhibiting an initially increasing trend, followed by a subsequent decrease. The impact of TN, TP, COD and NH_4^+-N pollution reached a maximum within a 1 km study area, while the impact of NO_3N reached a maximum at a buffer zone scale of 500 m, which may be due to the relatively singular land-use type within the small-scale buffer zone (200 m, 500 m). Within the large-scale buffer zone (5 km, 10 km), organic pollutants (COD) and inorganic pollutants (nitrogen and phosphorus) were easily absorbed by soil particles, allowing them to be utilized by vegetation or transformed into gas (such as nitrification and denitrification) or other insoluble substances (such as low-solubility or insoluble phosphate) during the transport process. This shows that optimizing small-scale spatial land-use patterns is of high significance to the overall quality of water within the Huaihe

River Basin.

4 Conclusions

(1) The surface water environment is closely related to land-use. The concentrations of TN, TP, COD, NH_4^+-N, NO_3^--N and the Nemerow index values were significantly positively correlated with cultivated land, wetlands and construction land, while a significant negative correlation was observed with forest land and grassland. In summary, crop land, wetlands, and Construction land are significant contributors to water pollution during winter, whereas woodlands and grasslands exhibit notable mitigating effects on water pollution. Therefore, in the context of land management and water resource protection, rational planning of land use, including increasing the coverage of woodlands and grasslands while curbing the expansion of cultivated land and built-up areas, would be beneficial for enhancing surface water quality.(2) There was a significant correlation observed between land-use patterns and water quality parameters at different buffer zone scales. Among them, land-use patterns within the 1 km buffer zone had the greatest impact of TN, TP, COD, NH_4^+-N and the Nemerow index, the R^2 values generated from the multiple regression model reaching 0.414, 0.36, 0.468, 0.254 and 0.563, respectively ($P < 0.01$). while land-use patterns within the 500 m buffer zone had the greatest impact on NO_3^-N, the R^2 values generated from the multiple regression model reaching 0.224 ($P < 0.01$). These results highlight the importance of optimizing land-use patterns within a 1 km area, in order to effectively protect water resources within the Huaihe River Basin.

Taking the Huai River Basin as the study area, this research preliminarily analyzes the impact of land use types on water quality within circular buffer zones, which may provide certain reference value for land use planning and water quality protection in the basin. Future studies could further integrate hydrological models and ecosystem models to simulate the responses of the water environment under different land use scenarios, offering more precise decision-making support for watershed management. Additionally, interdisciplinary collaboration should be strengthened to comprehensively consider the impacts of climate change and socio-economic factors on land use and the water environment, thereby constructing a more holistic watershed management framework.

Funding

This research was supported by Anhui Provincial Key Research and Development Project(The Ecological Environment Special Project)（NO.202004i07020012）

Reference

Bouchareb, N., Khammar, H., Bousbia, S., Lefilef, A., Boudeffa, K., Akboudj, A., Chardib, M., Bouguenna, R. (2024) Anthropogenic Influence and Climate Change: Water and Nutrient Dynamics in the Kebir-Rhumel Basin, (Northeastern Algeria). Global Nest Journal 26.

Chen, D., Elhadj, A., Xu, H., Xu, X., Qiao, Z. (2020) A study on the relationship between land use change and water quality of the Mitidja watershed in Algeria based on GIS and RS. Sustainability 12, 3510.

Dai, M.-J., Zhang, B., Du, Q.-Q., Sun, J.-H., Tian, L., Wang, Y.-D. (2024) Effects of Land Use Types on Water Quality at Different Buffer Scales: Tianjin Section of the Haihe River Basin as an Example. Huan jing ke xue= Huanjing kexue 45, 1512-1524.

Goodarzi, M.R., Niknam, A.R.R., Rahmati, S.H., Attar, N.F. (2023) Assessing land use changes' effect on river water quality in the Dez Basin using land change modeler. Environmental Monitoring and Assessment 195.

He, G., Fu, Y., Zhao, S. (2023) Evaluation of water ecological security in Huaihe River Basin based on the DPSIR-EES-SMI-P model. Water Supply 23, 1127-1143.

Hong, C., Xiaode, Z., Mengjing, G., Wei, W. (2016) Land use change and its effects on water quality in typical inland lake of arid area in China. Journal of Environmental Biology 37, 603-609.

Kamaruddin, A.F., Toriman, M.E., Juahir, H., Zain, S.M., Rahman, M.N.A., Kamarudin, M.K.A., Azid, A. (2015) Spatial characterization and identification sources of pollution using multivariate analysis at Terengganu river basin, Malaysia. Jurnal Teknologi 77.

Li, S., Peng, S., Jin, B., Zhou, J., Li, Y. (2019) Multi-scale relationship between land use/land cover types and water quality in different pollution source areas in Fuxian Lake Basin. Peerj 7.

Liang, J., Pan, S., Chen, W., Li, J., Zhou, T. (2021) Cultivated land fragmentation and its influencing factors detection: A case study in Huaihe River Basin, China. International Journal of Environmental Research Public Health 19, 138.

Mahdiani, H., Safari, S., Salehi, M.E. (2016) Fast and accurate FPGA-based framework for processor architecture vulnerability analysis. Integration 53, 14-26.

Maruthai, Rajendran , S., Raveena Selvanarayanan, S, G. (2025) Wastewater Recycling Integration with IoT Sensor Vision for Real-time Monitoring and Transforming Polluted Ponds into Clean Ponds using HG-RNN. Global Nest Journal 27, 1-11.

Mu, M., Gao, L., Zhang, H., Ge, J., Zhang, Z., Qiu, Y., Zhao, X. (2023) Effects of land use on water quality at different spatial scales in the middle reaches of Huaihe River. Journal of Freshwater Ecology 38, 2176373.

Prasad, D.V.V., Venkataramana, L.Y., Vikram, V., Vyshali, S., Shriya, B. (2024) Water quality prediction using statistical, ensemble and hybrid models. Global Nest Journal 26.

Selvanarayanan, Rajendran , S., Pappa, C.K., Thomas, B. (2024) Wastewater Recycling to Enhance Environmental Quality using Fuzzy Embedded with RNN-IoT for Sustainable Coffee Farming. Global Nest Journal 26.

Su, K., Wang, Q., Li, L., Cao, R., Xi, Y. (2022a) Water quality assessment of Lugu Lake based on Nemerow pollution index method. Scientific Reports 12.

Su, K., Wang, Q., Li, L., Cao, R., Xi, Y., Li, G. (2022b) Water quality assessment based on Nemerow pollution index method: A case study of Heilongtan reservoir in central Sichuan province, China. Plos One 17.

Tan, J., Xiong, L.-J., Wang, Q., Ren, Z.-W., Zhu, D.-D., Wang, M. (2024) Effects of Land Use Structure and Spatial Pattern at Different Temporal and Spatial Scales on Water Quality in Suzhou Creek. Huan jing ke xue= Huanjing kexue 45, 768-779.

Venkatraman, M., Surendran R., Senduru Srinivasulu, K, V. (2025) Water quality prediction and classification using Attention based Deep Differential RecurFlowNet with Logistic Giant Armadillo Optimization. Global Nest Journal 27, 1-13.

Wang, H., Xiong, X., Wang, K., Li, X., Hu, H., Li, Q., Yin, H., Wu, C. (2023a) The effects of land use on water quality of alpine rivers: A case study in Qilian Mountain, China. Science of the Total Environment 875.

Wang, L., Han, X., Zhang, Y., Zhang, Q., Wan, X., Liang, T., Song, H., Bolan, N., Shaheen, S.M., White, J.R., Rinklebe, J. (2023b) Impacts of land uses on spatio-temporal variations of seasonal water quality in a regulated river basin, Huai River, China. Science of the Total Environment 857.

Wang, X.-j., Zhang, J.-y., Shahid, S., Bi, S.-h., Elmahdi, A., Liao, C.-h., Li, Y.-d. (2018) Forecasting industrial water demand in Huaihe River Basin due to environmental changes. Mitigation Adaptation Strategies for Global Change 23, 469-483.

Wang, Y.-B., Junaid, M., Deng, J.-Y., Tang, Q.-P., Luo, L., Xie, Z.-Y., Pei, D.-S. (2024) Effects of land-use patterns on seasonal water quality at multiple spatial scales in the Jialing River, Chongqing, China. Catena 234, 107646.

Wang, Y., Sun, W., Zhao, Y., He, P., Wang, L., Nguyen, L.T.T. (2022) Assessment of Heavy Metal Pollution Characteristics andEcological Risk in Soils around a Rare Earth Mine in Gannan. Scientific Programming 2022.

Wu, J., Zeng, S., Yang, L., Ren, Y., Xia, J. (2021) Spatiotemporal Characteristics of the Water Quality and Its Multiscale Relationship with Land Use in the Yangtze River Basin. Remote Sensing 13.

Xiao-Mei, H., Jin, Y., Chao, L., Xiao-Jun, F., Yuan, Z. (2023) Impact of watershed habitat quality based on land use: a case study of taking Ciyao River Basin. Quality Assurance Safety of Crops Foods 15, 18-31.

Xu, D., Liu, D., Yan, Z., Ren, S., Xu, Q. (2023) Spatiotemporal variation characteristics of precipitation in the Huaihe River Basin, China, as a result of climate change. Water 15, 181.

Xu, G., Ren, X., Yang, Z., Long, H., Xiao, J. (2019a) Influence of Landscape Structures on Water Quality at Multiple Temporal and Spatial Scales: A Case Study of Wujiang River Watershed in Guizhou. Water 11.

Xu, Q., Wang, P., Shu, W., Ding, M., Zhang, H. (2021) Influence of landscape structures on river water quality at multiple spatial scales: A case study of the Yuan river watershed, China. Ecological Indicators 121.

Xu, Z., Pan, B., Han, M., Zhu, J., Tian, L. (2019b) Spatial–temporal distribution of rainfall erosivity, erosivity density and correlation with El Niño–Southern Oscillation in the Huaihe River Basin, China. Ecological Informatics 52, 14-25.

Yang, Y., Huang, X., Wu, X.-q., Liu, C.-r., Zhao, S.-y., Zhu, X.-h. (2023) The spatiotemporal variations characteristic and pollution evaluation of water quality in Qujiang River, China. Applied Water Science 13.

Yao, S., Chen, C., He, M., Cui, Z., Mo, K., Pang, R., Chen, Q. (2023) Land use as an important indicator for water quality prediction in a region under rapid urbanization. Ecological Indicators 146.

Zhang, L., Liu, X., Wei, H., Yang, C., Li, E., Wang, Z. (2022) Impact of land use on surface water quality: a case study of active agriculturally disturbed basin in China. International Journal of Environmental Science and Technology 19, 4435-4446.

Zhang, M., Rong, G., Han, A., Riao, D., Liu, X., Zhang, J., Tong, Z. (2021) Spatial-Temporal Change of Land Use and Its Impact on Water Quality of East-Liao River Basin from 2000 to 2020. Water 13.

Zhang, Y., Zhao, Y., Zhang, H., Cao, J., Chen, J., Su, C., Chen, Y. (2023) The Impact of Land-Use Composition and Landscape Pattern on Water Quality at Different Spatial Scales in the Dan River Basin, Qin Ling Mountains. Water 15.

Lllustration list

Figure 1 Map of the study area, showing the land-use map and sampling point distribution 5

Figure 2 The relative proportion of land-use types within the study area at different buffer zone scales 8

Figure 3 Distribution of pollutant concentrations and water quality index parameters at sampling points across the Huaihe River Basin study area 10

Figure 4 Nemerow pollution index value distribution throughout the Huaihe River Basin 11

Figure 5 The explanatory power of different water quality parameters based on the multiple linear regression model (R^2 value) data for land-use patterns at different buffer zone scales. 15

Schedule list

Table 1 Determination method used for each water quality index parameter............................. 4

Table 2 Laboratory Instruments 4

Table 3 Water quality level based on Nemerow pollution index method 7

Table 4 Descriptive statistics for water quality indicators in the ($mg \cdot L^{-1}$) 9

Table 5 Relationships between water quality parameters and land-use types at various buffer zone scales, based on Spearman's rank correlation coefficient data.................................. 13